

Defense Against Model Stealing Based on Account-Aware Distribution Discrepancy

Jian-Ping Mei^{1*}, Weibin Zhang^{1†}, Jie Chen^{1†}, Xuyun Zhang², Tiantian Zhu¹

¹College of Computer Science and Technology, Zhejiang University of Technology, Hangzhou, 310023 China

²School of Computing, Macquarie University, 4 Research Park Drive, Macquarie Park, NSW 2109

{jpmei, ttzhu}@zjut.edu.cn, zhangweibin30@gmail.com, chenjie.plus@qq.com, xuyun.zhang@mq.edu.au.

Abstract

Malicious users attempt to replicate commercial models functionally at low cost by training a clone model with query responses. It is challenging to timely prevent such model-stealing attacks to achieve strong protection and maintain utility. In this paper, we propose a novel non-parametric detector called Account-aware Distribution Discrepancy (ADD) to recognize queries from malicious users by leveraging account-wise local dependency. We formulate each class as a Multivariate Normal distribution (MVN) in the feature space and measure the malicious score as the sum of weighted class-wise distribution discrepancy. The ADD detector is combined with random-based prediction poisoning to yield a plug-and-play defense module named D-ADD for image classification models. Results of extensive experimental studies show that D-ADD achieves strong defense against different types of attacks with little interference in serving benign users for both soft and hard-label settings. Codes are available from <https://github.com/AI-EXP-group/D-ADD>.

Introduction

Deep neural networks that are trained on large-scale datasets have become essential tools in many machine learning tasks, especially in image classification (Krizhevsky, Sutskever, and Hinton 2017; Kolesnikov et al. 2020; Redmon and Farhadi 2018), where they have achieved state-of-the-art performance. However, training a powerful neural network model with a large number of parameters requires significant data and computation resources. As a result, companies that own the intellectual property of these models offer cloud-based services through APIs to generate profits. For instance, Google Cloud Vision API¹ provides a chargeable service for retrieving image category information through API queries. Unfortunately, when providing such services, the models to be queried are exposed to the risk of theft. Competitors or malicious users may be able to clone a model with comparable performance at a low cost and use it as a substitute for the target model functionally (Truong et al. 2021; Orekondy, Schiele, and Fritz 2019; Barbalau et al. 2020; Sanyal, Addepalli, and Babu 2022; Tramèr et al. 2016). This is known as “model stealing”. A stealer makes

use of the labeling service to annotate a set of query images, and use them to train their own models. Model stealing could infringe on the commercial profit of the original service providers and even bring unfair market competition. It also poses threats to confidentiality as well as functionality if the stolen model is used as an auxiliary tool to carry out other inferential or adversarial attacks (Goodfellow, Shlens, and Szegedy 2015).

To mitigate the risk of model theft, labeling services are provided in a *black-box* manner, meaning that visitors are not provided with any internal details of the model or its training process. The only information that is returned in response to each query is a single class label (i.e., hard label) or a probability distribution over all the classes (i.e., soft label). Malicious users are assumed to have no or very limited in-distribution data as model stealing becomes unnecessary if they have enough samples from the original training distribution. Under the *data-limited* condition, attackers resort to querying with surrogate samples or model generated examples. Despite the fundamental protection provided by the black box and hard-label setting, it is still vulnerable to various model extraction attacks. It has reported in (Sanyal, Addepalli, and Babu 2022) that even in the hard label and black-box setting, their attack can achieve about 93% performance of the target models on CIFAR-10 and CIFAR-100.

Various approaches have been proposed for defending against model stealing, but their limited defense capability and high deployment costs restrict them from practical use. A well performing malicious detector is a prerequisite for enabling strong defense. Most existing detection-based defense approaches evaluate each query individually to predict whether it is “malicious” or “benign” (Kariyappa and Qureshi 2020; Kariyappa, Prakash, and Qureshi 2021b; Zhang et al. 2023b). However, query-wise detection is challenging for practical situations where some queries from benign users appear to be malicious while some attack queries are benign-looking. Moreover, learning a good discrimination ability often requires to collect enough malicious samples of various attacks.

In this paper, we propose a new method to detect queries from malicious users using a technique called Account-aware Distribution Discrepancy (ADD). Our method measures the discrepancy between the query and training distributions using window-augmented feature statistics. By com-

*Corresponding author.

†These authors contributed equally.

¹<https://cloud.google.com/vision/docs/labels>

binning the ADD detector with random-based prediction poisoning, we have a powerful defense module named D-ADD with the following advantages:

- **A wide range of applications.** It provides strong defense and high utility against different types of attacks for both soft and hard label settings.
- **Low cost.** It is training-free and require no known malicious data.
- **Deployment convenience.** It works in a plug-and-play manner, and causes negligible response latency.

We have conducted extensive empirical evaluations with various settings to verify its detection performance, defense capability for protecting image classification models from model stealing, as well as robustness to adaptive attack.

Related Work

Black-box model stealing attacks

Black-box model stealing refers to a technique where malicious users attempt to functionally copy a target model without having any knowledge or access to its weights, architecture, training data, or intermediate results. A stolen or clone model is sometime created to assist with black-box adversarial example generation (Yu et al. 2020). These adversarial attacks start with a small number of seed images from the target model’s training dataset, and then synthesize examples by iteratively adding imperceptible perturbations using techniques such as JBDA (Papernot et al. 2017) and its variants (Juuti et al. 2019). Since the direct purpose of this type of attacks is to approximate the decision boundaries of the target model instead of functional replication, models cloned with adversarial attacks have much lower classification accuracy compared to other attacks (Papernot et al. 2017). In this paper, we consider model-stealing with the goal of creating a low-cost functionality clone of a target image classification model.

Model-stealing attackers typically have little or no access to the proprietary training data of the target model. To handle this data-limited situation, attackers use surrogate or model-generated data as queries. Using substitute samples as queries, the KnockoffNets attack comes to be a strong baseline if the surrogate dataset has high semantic or distributional similarity to the training data (Orekondy, Schiele, and Fritz 2019). Other studies borrow ideas from data-free knowledge distillation to steal with queries synthesized by maximizing prediction confidence (Barbalau et al. 2020) or the output discrepancy between the target and clone models (Kariyappa, Prakash, and Qureshi 2021a; Truong et al. 2021). The DFMS attack in (Sanyal, Addepalli, and Babu 2022) has been shown to achieve high clone model performance with hard labels.

Defense against black-box model stealing

Defense approaches can be broadly categorized into two groups based on whether they perform maliciousness evaluation. Some approaches apply perturbation injection indiscriminately to poison any returned response (Lee et al. 2018). Perturbations are learned based on certain objectives,

such as maximizing the clone model’s training loss or restricting predictions near the decision boundary, and can be injected into the final predictions (Orekondy, Schiele, and Fritz 2020; Mazeika, Li, and Forsyth 2022), inputs (Zhang et al. 2023a), or outputs of intermediate layers (Lee, Han, and Lee 2022). These approaches aim to reduce knowledge leakage from the returned label without significantly impacting the utility for benign users. Although later approaches like Prediction Poisoning (PP) (Orekondy, Schiele, and Fritz 2020) can tolerate higher levels of perturbations by sacrificing some level of utility, poisoning must still be limited due to their indiscriminate nature, which leads to minimal protection especially for attacks working with hard labels.

For defense approaches that perform poisoning only to suspicious queries, the identification of queries from malicious users becomes critical. Many of these approaches evaluate each query individually to predict whether it is “malicious” or “benign” using a detector learned from known malicious queries (Kariyappa and Qureshi 2020; Kariyappa, Prakash, and Qureshi 2021b; Zhang et al. 2023b). However, the final performance of these approaches is not guaranteed when the malicious query set they learn from is limited in scale and coverage due to the high collection cost.

Some other studies proposed defense methods for specific types of model extraction attacks. For example, stateful detection approaches such as PRADA are particularly tailored for the detection of adversarial example generation, where the query sequence consists of images with high self-similarity visually (Chen, Carlini, and Wagner 2020; Juuti et al. 2019), and the retraining based defense works only for data-free model extraction attack (Wang et al. 2023).

Threat Model

Black-box labeling service. The API-based labeling service with a high-performance image classification model is provided to registered users in a black-box manner. The defender is aware of the account information that each query is submitted. The target model consists of an encoder $g_\theta(\cdot)$ and a classifier head $f_\phi(\cdot)$. For any given query image \mathbf{x} , the model returns a class label $\mathbf{y} = f_\phi(g_\theta(\mathbf{x}))$, i.e., a vector \mathbf{y} of length K . The label is said to be “soft” if it contains probabilities of all the K classes, and “hard” if it is one-hot.

Goals of the attacker and the defender. The attackers’ goal is to train a clone model with comparable classification performance to the target model using label information returned by querying the target model. The defender’s goal is to create a defense mechanism that stops leaking positive knowledge learned by the service model to malicious users, or specifically, minimizing the performance of the stolen model while having little impact on normal user experience.

Data availability. It is typical that all users have no access to the original training data of the target model as the data itself may be the most important property that its owner want to protect. Nevertheless, the fundamental assumption stated below is necessary to make the detection issue solvable.

Fundamental assumption: *queries from benign users are overall with larger semantic similarities to the training data than those from malicious users, and the target encoder is able to capture the semantic gap.*

Defense with Account-aware Distribution Distance (D-ADD)

Although non-parametric detectors are attractive for their simplicity in concept as well as deployment, existing ones are not effective enough to provide robust protection against various stealing attacks. One straightforward method is to apply out-of-distribution (OOD) detection metrics, such as confidence (Hendrycks and Gimpel 2016) or energy (Liu et al. 2020) by treating in-distribution (ID) samples as benign queries and OOD samples as malicious ones. Since some legitimate user queries may differ even more from the training examples than attack queries, query-wise detectors result in false-alarms for those low-quality benign queries.

In this paper, we further exploit the potential of detection-based defense by proposing a new method called D-ADD. It is comprised of two main components: an Account-aware Distribution Distance (ADD) detector and a random-based prediction poisoning step as illustrated in Fig. 1. A randomly selected label is returned to mislead clone model training if the query is found to be from a malicious user. The decoupling formulation with the target model allows for seamless integration and removal of this defense module. Since the poisoning strategy used here is quite straightforward, we focus on the malicious detector.

The ADD malicious detector

Overview. The proposed ADD detector works in the output space of the target encoder. As sketched on the right of Fig. 1, it attempts to recognize whether a query is submitted by a malicious account, by comparing query distribution with the training data distribution in the embedding space. Drawing inspiration from data-free knowledge distillation (Choi et al. 2020), we assume that feature statistics of each class follow a Multi-Variate Normal (MVN) distribution $\mathcal{N}(\boldsymbol{\mu}, \boldsymbol{\Sigma})$.

Formulation. To get a reference distribution of each class, we store the mean vector and covariance matrix for each of the K classes based on features of training samples in that class. A sliding window is allocated and maintained for each account to store features of a number of latest queries. The stored features of the corresponding account are retrieved to enlarge the coming queries to obtain more reliable statistical information.

Given the window-augmented query batch Q , we partition them into C groups according to their predicted classes, i.e., $Q = \mathcal{X}_1 \cup \mathcal{X}_2 \dots \mathcal{X}_C$, where the subset \mathcal{X}_c contains features of queries that predicted to be in the c th class. We then calculate the mean vector $\boldsymbol{\mu}_c^a$ and covariance matrix $\boldsymbol{\Sigma}_c^a$ with \mathcal{X}_c , and measure the class-wise discrepancy based on the distance between the two distributions of this class, i.e.,

$$\begin{aligned} d_c(\boldsymbol{\mu}_c^r, \boldsymbol{\Sigma}_c^r, \boldsymbol{\mu}_c^a, \boldsymbol{\Sigma}_c^a) &= \text{dist}(\mathcal{N}_c^r(\boldsymbol{\mu}_c^r, \boldsymbol{\Sigma}_c^r), \mathcal{N}_c^a(\boldsymbol{\mu}_c^a, \boldsymbol{\Sigma}_c^a)) \\ &= \|\boldsymbol{\mu}_c^r - \boldsymbol{\mu}_c^a\|^2 + \text{tr} \left[\boldsymbol{\Sigma}_c^r + \boldsymbol{\Sigma}_c^a - 2(\boldsymbol{\Sigma}_c^r \boldsymbol{\Sigma}_c^a)^{\frac{1}{2}} \right]. \end{aligned} \quad (1)$$

where $\text{dist}(\mathcal{N}_c^r, \mathcal{N}_c^a)$ denotes the squared Fréchet distance between the reference and the query-batch distribution of class c .

The final Malicious Score (MS) for the query batch Q is then calculated as the sum of weighted class-wise distance over all the C classes, i.e.,

$$MS_{ADD}(Q) = \sum_{c \in \mathcal{C}} \frac{|\mathcal{X}_c|}{N} d_c(\boldsymbol{\mu}_c^r, \boldsymbol{\Sigma}_c^r, \boldsymbol{\mu}_c^a, \boldsymbol{\Sigma}_c^a). \quad (2)$$

The larger the MS, the more possible that the current query batch is from a malicious user. Here each batch may only involve a subset of the K classes, i.e., $C \leq K$. Fig.2 illustrates the ability of ADD to detect benign-looking malicious queries and malicious-looking benign queries.

Complexity and storage overhead. ADD is training-free. Given window size N and embedding dimension d , the time complexity of straightforward implementation for calculating a covariance matrix is $O(Nd^2)$ and multiplication of two covariance matrices in the Fréchet distance is $O(d^3)$. Since both N and d are typically less than one thousand, the time complexity is small. In our experiment, the response latency caused by defense is less than 5ms per query.

Low-dimensional features instead of original images are stored. The storage overhead required to allocate each account a small window is negligible for modern cloud-based servers. For instance, storing 64 features, each of which is a 256-dimensional floating-point vector would require 64KB. This means that it is possible to accommodate up to 16,384 users simultaneously with 1GB of storage space.

Discussions

Advantages over simplified variants

In our default formulation in Eq.(2), the malicious score of a given query batch is the sum of weighted class-wise distances of feature statistics. For each involved class of the query batch, a distance is calculated to measure its deviation to the corresponding reference class, and is weighted by the size of this class. Next, we consider two possible variants.

Equal Weights (EW). Each class is equally weighted when calculating the total distance, i.e.,

$$MS_{EW}(Q) = \sum_{c \in \mathcal{C}} d_c(\boldsymbol{\mu}_c^r, \boldsymbol{\Sigma}_c^r, \boldsymbol{\mu}_c^a, \boldsymbol{\Sigma}_c^a). \quad (3)$$

Global Distribution Distance (GDD). The feature statistics are calculated based on the global distribution without considering each class individually, i.e.,

$$MS_{GDD}(Q) = d(\boldsymbol{\mu}^r, \boldsymbol{\Sigma}^r, \boldsymbol{\mu}^a, \boldsymbol{\Sigma}^a) \quad (4)$$

where $\boldsymbol{\mu}^r$ and $\boldsymbol{\Sigma}^r$ are the mean and covariance matrix calculated based on all the training samples, and $\boldsymbol{\mu}^a$ and $\boldsymbol{\Sigma}^a$ are calculated based on all query features in Q .

As evidenced by experimental results, both class-conditional and weight by class size are crucial for enabling ADD to handle more challenging situations, where queries from benign users are not strictly in-distribution but exhibit various types of distribution shifts.

Robustness to adaptive attack

Attackers can try to evade a defense technique once they understand its working principle. In our case, the attacker may

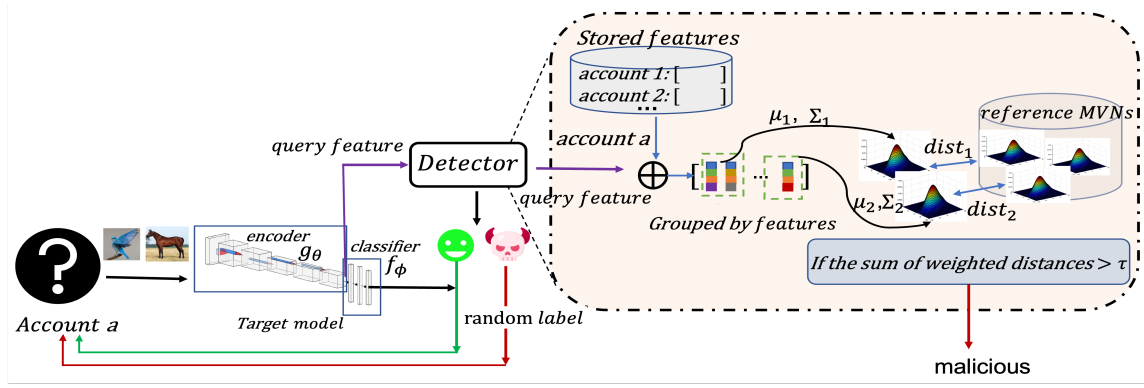


Figure 1: Overall pipe line of the proposed D-ADD Defense. The main idea of the new embedding space detector ADD is sketched on the right.

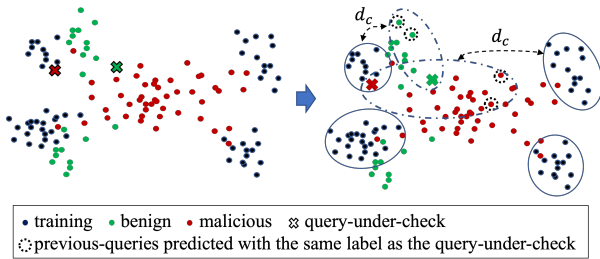


Figure 2: Illustration of the working principle of the proposed ADD detector.

manipulate the query stream by mixing benign-looking samples into the window to tweak the batch-based query distribution towards a benign one so that the whole batch will be incorrectly labeled as benign. While combing more benign-looking samples makes it easier to evade ADD, the attacker is assumed to have very limited access to such kind of data.

Smaller window leads to more robustness. Assume that the attacker has H benign-looking (BL) samples and abundant malicious-looking (ML) samples, and has the knowledge of the minimum percentage of BL in each window required to evade ADD is $x\%$, but unaware of the window size. We consider the attack query sequence with a length of $H \times (1 + M)$ is organized with each single BL sample followed by M ML samples, where $M = \lceil 100/x \rceil - 1$. Noting that this is the maximum value of M that ensures the overall percentage of BL queries in the sequence is at least $x\%$. The uniform mixing-up of BL and ML throughout the sequence leads to the largest number of subsequences with a BL percentage not less than $x\%$.

Based on the above attack sequence, we can derive that the number of malicious queries including BL and ML that missed by ADD is related to window size N , i.e.,

$$no.missed = \begin{cases} \overbrace{(1 + N - 1)}^{BL} \times H & \text{for } N \leq M \\ \overbrace{(1 + M)}^{BL} \times H & \text{for } N \geq M + 1 \end{cases}$$

Detection vs. robustness. A large window gives more reliable statistics and we are even able to implicitly realize an infinitely large window ($N \rightarrow \infty$) by incrementally updating the statistics. Nevertheless, a small window provides more sensitivity to changes in query sequences and leads to more robustness as shown in the above formula.

Benefits of detection in embedding space

As a commercialized service provider, the target model is expected to have been trained to generalize to distribution shifts caused by input-space perturbations like changes of background, resolution, etc. This gives the following benefits by working as an embedding space detector. It allows ADD maintain good utility when queries from benign users are not strictly in-distribution. Moreover, when an attacker tries to evade ADD by increasing the percentage of benign-looking samples via duplication or augmentation, we can detect such behavior by observing abnormally high occurrence of very similar features. This should work especially well for encoders trained by contrastive learning, which maps augmented inputs of the same image to be closer to each other than those of different images (Chen et al. 2020).

Experiments-I: Malicious Detection

We first evaluate the performance of the ADD detector, study the impact of window size, and also compare with two simplified variants.

Settings

Target models and malicious queries. Following (Kariyappa, Prakash, and Qureshi 2021b), we have trained five target models on well-known image datasets, namely MNIST, FashionMNIST, CIFAR-10, CIFAR-100, and Flower-17 for image classification. We follow (Kariyappa and Qureshi 2020) to set model architectures and surrogate data to simulate malicious queries (given in Table A1).

benign queries. We evaluate the performance of each detector in two scenarios. In this first scenario, benign users have *in-distribution* queries. For each target model, we

Scenario-1: in-distribution benign queries

training data	benign vs. malicious	FPR@TPR95(\downarrow)(%)				AUROC(\uparrow)(%)				AUPR(\uparrow)(%)			
		Baseline	Energy	PRADA	ADD(N)	Baseline	Energy	PRADA	ADD(N)	Baseline	Energy	PRADA	ADD(N)
MNIST	MNIST vs. FashionMNIST	5.26	2.16	95.64	0.00 (8)	98.65	99.53	63.04	100.00 (8)	99.71	99.91	88.26	100.00 (8)
FashionMNIST	FashionMNIST vs. MNIST	90.56	91.78	95.24	0.00 (8)	59.90	71.04	50.00	100.00 (8)	89.76	94.18	50.00	100.00 (8)
CIFAR-10	CIFAR-10 vs. CIFAR-100	34.46	35.47	95.52	0.00 (8)	89.14	90.45	41.80	100.00 (8)	96.84	97.42	79.46	100.00 (8)
CIFAR-100	CIFAR-100 vs. CIFAR-10	60.14	65.17	70.21	11.11 (256)	76.79	77.19	85.52	97.93 (256)	92.72	92.96	97.30	99.59 (256)
Flower-17	Flower-17 vs. Indoor-67	51.18	63.53	17.65	0.00 (32)	84.41	87.57	97.50	99.97 (32)	99.76	99.82	99.05	99.98 (32)

Scenario-2: benign queries from distribution with shifts

training data	benign vs. malicious	FPR@TPR95(\downarrow)(%)				AUROC(\uparrow)(%)				AUPR(\uparrow)(%)			
		Baseline	Energy	PRADA	ADD(N)	Baseline	Energy	PRADA	ADD(N)	Baseline	Energy	PRADA	ADD(N)
MNIST	USPS-10 vs. FashionMNIST	56.81	53.08	100.00	8.04 (16)	81.89	83.11	34.84	98.12 (16)	96.56	96.84	84.69	99.89 (16)
	USPS-7 vs. FashionMNIST	56.96	53.19	98.03	12.51 (16)	81.82	83.06	56.90	97.84 (16)	97.56	97.76	93.31	99.91 (16)
	USPS-3 vs. FashionMNIST	57.58	53.66	25.11	14.47 (16)	81.55	82.86	96.89	97.64 (16)	98.94	99.03	99.82	99.96 (16)
CIFAR-10	STL-9 vs. CIFAR-100	57.80	58.11	49.20	1.07 (16)	77.41	80.21	91.26	99.76 (16)	96.56	97.14	99.19	99.98 (16)
	STL-7 vs. CIFAR-100	58.17	58.47	81.72	1.42 (16)	77.21	80.04	69.41	99.74 (16)	97.28	97.74	96.05	99.98 (16)
	STL-3 vs. CIFAR-100	57.72	58.92	20.43	1.83 (16)	76.84	79.85	97.50	99.65 (16)	98.79	99.01	99.93	99.99 (16)

Table 1: Comparison of different malicious detectors. The number in brackets is the window size N used in ADD.

use the corresponding testing set as benign queries. While this setting has been widely adopted in the literature, it is overly idealized since users typically do not have access to samples from the data distribution of the target model in real-world applications. Therefore, we further consider a more challenging scenario where benign queries exhibit *distribution shifts*. It occurs due to various perturbations in the input space, such as changes in background, corruption, and resolution. Distribution shift is also attributed to label distribution inconsistency, for instance, when users query with images from only a subset of classes rather than all the classes that the target model is trained on. Results are reported based on MNIST and CIFAR-10 models that we found suitable benign queries. For the MNIST model, we use samples from the USPS dataset as benign queries. USPS also contains images of ten digits like MNIST but collected from a different source, therefore exhibiting feature distribution shifts. To further consider label inconsistency, we extract USPS-7 and USPS-3 to contain images of seven or three randomly sampled digits, respectively. For the CIFAR-10 model, we use samples from the STL-10 dataset as benign queries. We discard the images of *monkey* from STL-10 as it is not included in CIFAR-10, leaving nine classes that appeared in both datasets. Similarly, another two subsets denoted as STL-7 and STL-3 are also used to simulate label distribution inconsistency.

Compared methods and Evaluation metrics. We compare ADD with three non-parametric detection approaches *Baseline* (Hendrycks and Gimpel 2016), *Energy* (Liu et al. 2020) and *PRADA* (Juuti et al. 2019). The detection is correct when a query from a **benign account** is labeled as **positive**, or a query from a **malicious account** is labeled as **negative**. Results are reported in terms of three widely used metrics. FPR@TPR95 (False Positive Rate at 95% True Positive Rate) indicates the percentage of negative samples that are mistakenly classified as positive ones given a True Positive Rate of 95%.

Results: comparison with others

Table 1 gives the results of four detectors. The corresponding window size is given in brackets after the result of ADD. It is seen that ADD performs consistently much better than

other approaches in both scenarios. The performances of *Baseline* and *Energy* are comparable. Both of them perform well only for the simple MNIST model. The results of PRADA confirms that it often fails to work properly against a wide range of attacks due to its formulation limitation mentioned earlier.

We found that ADD correctly recognized all the malicious queries from benign ones given a sufficiently large window. The perfect detection indicates that we are able to separate all malicious queries from benign ones, or all benign query batches have smaller scores than malicious ones calculated with the proposed measurement in Eq.(2). Detailed results on the impact of window size are given later. A larger window size is needed to achieve good detection in more complex situations when the quality of malicious queries are relatively high compared to benign ones. For example, CIFAR-10 is used to steal the CIFAR-100 model. Although the performance of ADD degrades to some degree compared to in-distribution benign queries with the same window size for difficult benign queries, it can still be remedied by using a larger window. In practice, a 100% detection rate may not be necessary, as a small number of false negatives may not provide sufficient information for effective model extraction.

Impact of window size on detection

Now, we study the impact of window size N on the separation of malicious scores between benign queries and malicious queries. Here results are obtained with in-distribution benign queries. Conclusions are the same for benign queries with distribution shifts. Fig. 3 plots the malicious scores of benign query batches (green dots) and malicious query batches (red dots) with various window sizes (Results of MNIST and Flower-17 provided in Appendix Fig.A3 are similar to FashionMNIST).

We observed that, a larger window size generally leads to a larger gap or a clearer separation between the scores of benign and malicious queries. While perfect detection can be achieved theoretically as long as no overlapping exists between the two sets of scores, a larger gap makes the selection of a proper threshold easier. For the more complex task of CIFAR-100, we are still able to achieve a reasonable degree of separation by increasing N .

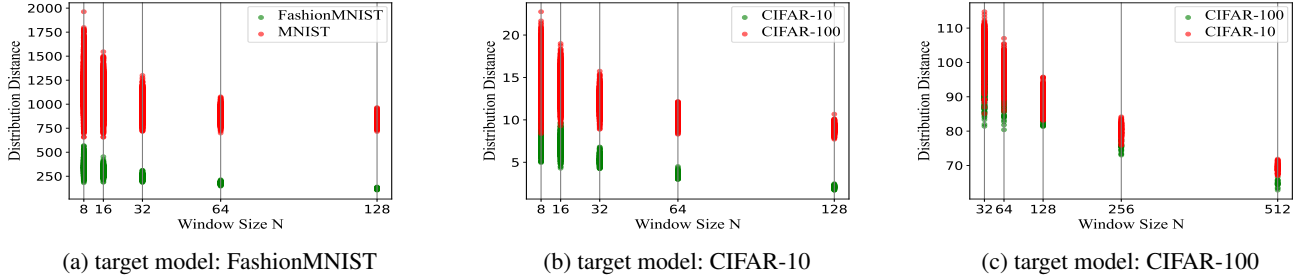


Figure 3: Impact of sliding window size N on distribution of Malicious Score (MS)s produced by ADD. Each red dot is calculated with a window of N randomly selected surrogate samples as malicious queries, and each green dot is calculated with N randomly selected testing images as benign queries.

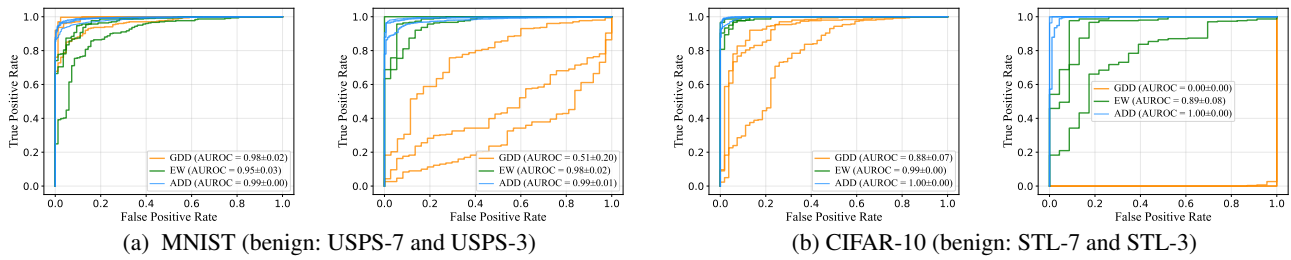


Figure 4: ROC curves of ADD and two simplified variants for MNIST (malicious: FashionMNIST) and CIFAR-10 (malicious: CIFAR-100). We repeat three times to generate the benign queries by randomly selecting a given number of classes.

Comparison with two simplified variants

Fig. 4 plots the ROC curves of the default ADD detector and its two simplified variants. We observe that the default formulation is more robust to distribution shifts than the other two by maintaining high AUROC values in all the cases. GDD is very sensitive to shifts caused by label inconsistency and performs poorly when benign queries only involves a small number of classes. This indicates the importance of measuring distribution distance in a class-conditional way. Weighting the class-wise distribution distance differently is also important to further improve the detection performance as shown by comparing EW and ADD.

Experiments-II: Model Stealing

We now assess the effectiveness of our proposed defense approach in safeguarding neural classifiers against three state-of-the-art functionality clone attacks.

Settings

Attacks. In our experiments, we assume that the attacker is aware of the architecture of the target model. This setting makes model stealing becomes easier while defense more challenging. It has been reported in (Kariyappa, Prakash, and Qureshi 2021b) that JBDA-type attacks have low clone model accuracy as they are designed to assist adversarial-example generation instead of functionality replication. Therefore, we here only consider KnockoffNets

(Orekondy, Schiele, and Fritz 2019) and two data-free attack methods: DFME (Truong et al. 2021) and DFMS (Sanyal, Addepalli, and Babu 2022).

Hyperparameter settings. For the proposed D-ADD defense, we set the training accuracy dropping ratio γ to 10^{-4} , the sliding window size N is set to 256 for CIFAR-100 and 64 for all others. Without loss of generality, we consider each user query contains one image. The clone model is trained using the SGD optimizer for 50 epochs with a cosine annealing schedule and an initial learning rate of 0.1.

Evaluation. The performance of target and clone classification models are evaluated using the most widely used Top-1 classification accuracy on the corresponding testing data. Following existing studies, we evaluate a defense approach against model stealing with respect to its impact on the performance of the target model and the clone model. Specifically, a smaller drop in accuracy of the target model for benign queries indicates higher *utility*, while a larger performance drop of the clone model in the target classification task demonstrates stronger *protection*.

Compared defense approaches. We compare D-ADD with state-of-the-art defense approaches, including AM(Kariyappa and Qureshi 2020), EDM (Kariyappa, Prakash, and Qureshi 2021b), CIP (Zhang et al. 2023b), and MeCo (Wang et al. 2023). The first three deal with KnockoffNets while the last one is designed for data-free attacks.

Dataset	clone model acc.(%)												
	target model (acc.%)		KnockoffNets (soft label)					DFME (soft label)			DFMS (hard label)		
	<i>undef</i>	<i>D-ADD</i> (acc. drop)	<i>undef</i>	<i>AM</i>	<i>EDM</i>	<i>CIP</i>	<i>D-ADD</i>	<i>undef</i>	<i>MeCo</i>	<i>D-ADD</i>	<i>undef</i>	<i>MeCo</i>	<i>D-ADD</i>
MNIST	99.21	99.21 (-0.00)	97.23	83.5	51.34	87.23	12.08	98.85	79.98	10.28	97.95	98.39	10.12
FashionMNIST	86.08	86.08 (-0.00)	48.67	27.5	15.28	31.42	10.15	87.51	70.20	10.23	73.78	74.51	10.34
CIFAR-10	94.27	94.27 (-0.00)	87.11	77.2	68.50	75.59	10.29	91.12	77.25	10.46	89.01	80.51	10.86
CIFAR-100	74.53	74.44 (-0.09)	49.31	51.0	41.16	32.77	5.22	52.27	22.12	1.13	68.71	65.85	1.30
Flowers-17	88.82	88.82 (-0.00)	82.35	27.2	30.15	12.93	5.88	64.12	27.06	5.93	67.05	60.48	5.67

Table 2: Comparison with existing defense methods against different attacks.

Results

Table 2 compares the performance of different defense methods against three attacks. It is seen from the results of undefended clone model that KnockoffNets performs well with proper surrogate data. DFME and DFMS achieve stable performance without using any natural-image queries but at a larger query cost compared to KnockoffNets.

The clone model accuracy drops when defense is applied. Compared to other approaches, D-ADD achieves significantly better defense capability. In all cases, the clone model’s performance approaches the level of a random classifier when D-ADD is employed. While working with hard labels enables the DFMS attack to perfectly evade detection-free defense approaches including MeCo, the protection of D-ADD remains the same like soft label settings.

As seen from the second and third columns, performance of the target models is largely preserved when D-ADD is applied, with less than 0.1% accuracy drop for the worst case.

Experiments-III: Adaptive Attacks

Finally, we provide empirical results to show the capability of D-ADD in dealing with adaptive attacks.

Settings and evaluation. We consider that the attacker has a small number of in-distribution (ID) samples as benign-looking images, which are uniformly mixed with surrogate samples, so that the percentage of ID samples in a window is always close to the overall mix-up ratio. To evaluate the robustness of D-ADD, we compare the performance of the models *mix_clone* and *id_clone*. The *mix_clone* model is trained using all the queries, while the *id_clone* model is trained using the same set of ID queries only. The D-ADD defense is considered robust against this kind of adaptive attack if *mix_clone* performs better than *id_clone* with no defense but worse when D-ADD is employed, i.e., the following holds in term of accuracy:

$$undef(mix_clone) > id_clone > D-ADD(mix_clone)$$

The intuition is that the attacker would not pay extra cost for collecting and querying with OOD surrogate samples unless there is a significant accuracy gain.

To simulate this scenario, we performed an adaptive KnockoffNets attack by mixing queries in each sliding window with a certain mix-up ratio with a window size of 64. Generally, the more unique benign-looking samples are used as queries, the more likely that *id_clone* performs better than *mix_clone*. Based on the assumption of data limitation as well as the above condition, we limited the percentage of

Dataset	No. ID queries	<i>mix_clone</i> (acc.%)		<i>id_clone</i> (acc.%)
		<i>undef</i>	<i>D-ADD</i>	
MNIST	60	98.28	22.45	63.06
	600	98.58	24.83	88.82
FashionMNIST	60	63.32	14.11	41.07
	600	76.24	18.58	54.64
CIFAR-10	500	87.09	10.64	35.77
	5000	89.27	25.88	70.77
CIFAR-100	500	51.83	5.29	8.19
	5000	61.71	9.35	36.59
Flower-17	100	81.76	8.82	28.82
	500	85.88	15.88	61.17

Table 3: Robustness of D-ADD to adaptive attack.

benign-looking samples to be less than 10% of surrogate queries for CIFAR-10, CIFAR-100 and Flower-17, and less than 1% for other two simple tasks.

Results. Table 3 displays the test accuracy of clone models *mix_clone* and *id_clone*. It clearly shows that *mix_clone* outperforms *id_clone* in all cases when the target model is not protected with any defense technique. However, when D-ADD is employed, the accuracy of *mix_clone* becomes worse than *id_clone*. According to the evaluation criterion given earlier in this section, D-ADD effectively resists mixing-based adaptive attacks.

Conclusion

While real-time defense provides timely protection for the target model against stealing attacks, differentiating queries of malicious users from those submitted by benign users, which is the key to enable strong protection, is difficult in practical scenarios. We have investigated a new direction to design malicious detectors by leveraging local dependency between nearby queries in the stream from the same account, and instantiated this idea with a feature space non-parametric detector based on weighted class-wise distribution discrepancy. We provided analytical discussion and experimental evidence to show that the proposed defense provides an important complement to researches on model stealing defense. However, like other approaches, our approach’s detection and robustness are only ensured under certain circumstances. More efforts are needed in the future to make it more suitable for practical use. It is also important to consider integrating it with other defensive means to handle various risks in complex real-world scenarios such as advanced adaptive attacks and sybil attacks.

References

- Barbalau, A.; Cosma, A.; Ionescu, R. T.; and Popescu, M. 2020. Black-Box Ripper: Copying black-box models using generative evolutionary algorithms. *Annual Conference on Neural Information Processing Systems*, 33: 20120–20129.
- Chen, S.; Carlini, N.; and Wagner, D. A. 2020. Stateful Detection of Black-Box Adversarial Attacks. In *ACM Workshop on Security and Privacy on Artificial Intelligence*.
- Chen, T.; Kornblith, S.; Norouzi, M.; and Hinton, G. E. 2020. A Simple Framework for Contrastive Learning of Visual Representations. In *International Conference on Machine Learning*, volume 119, 1597–1607.
- Choi, Y.; Choi, J.; El-Khamy, M.; and Lee, J. 2020. Data-free network quantization with adversarial knowledge distillation. In *Proceedings of the IEEE/CVF Conference on Computer Vision and Pattern Recognition Workshops*, 710–711.
- Goodfellow, I. J.; Shlens, J.; and Szegedy, C. 2015. Explaining and Harnessing Adversarial Examples. In *Proceedings of the International Conference on Learning Representations*.
- Hendrycks, D.; and Gimpel, K. 2016. A baseline for detecting misclassified and out-of-distribution examples in neural networks. *arXiv preprint arXiv:1610.02136*.
- Juuti, M.; Szyller, S.; Marchal, S.; and Asokan, N. 2019. PRADA: protecting against DNN model stealing attacks. In *IEEE European Symposium on Security and Privacy (EuroS&P)*, 512–527.
- Kariyappa, S.; Prakash, A.; and Qureshi, M. K. 2021a. MAZE: Data-Free Model Stealing Attack Using Zeroth-Order Gradient Estimation. In *Proceedings of the IEEE Conference on Computer Vision and Pattern Recognition*, 13814–13823.
- Kariyappa, S.; Prakash, A.; and Qureshi, M. K. 2021b. Protecting DNNs from theft using an ensemble of diverse models. In *Proceedings of the International Conference on Learning Representations*.
- Kariyappa, S.; and Qureshi, M. K. 2020. Defending against model stealing attacks with adaptive misinformation. In *Proceedings of the IEEE/CVF Conference on Computer Vision and Pattern Recognition*, 770–778.
- Kolesnikov, A.; Beyler, L.; Zhai, X.; Puigcerver, J.; Yung, J.; Gelly, S.; and Houlsby, N. 2020. Big transfer (bit): General visual representation learning. In *Proceedings of the European Conference on Computer Vision*, 491–507.
- Krizhevsky, A.; Sutskever, I.; and Hinton, G. E. 2017. ImageNet classification with deep convolutional neural networks. *Communications of the ACM*, 60(6): 84–90.
- Lee, J.; Han, S.; and Lee, S. 2022. Model Stealing Defense against Exploiting Information Leak through the Interpretation of Deep Neural Nets. In *Proceedings of the International Joint Conference on Artificial Intelligence*, 710–716.
- Lee, T.; Edwards, B.; Molloy, I.; and Su, D. 2018. Defending against model stealing attacks using deceptive perturbations. *arXiv preprint arXiv:1806.00054*.
- Liu, W.; Wang, X.; Owens, J. D.; and Li, Y. 2020. Energy-based Out-of-distribution Detection. In *Annual Conference on Neural Information Processing Systems*, volume 33, 21464–21475.
- Mazeika, M.; Li, B.; and Forsyth, D. A. 2022. How to Steer Your Adversary: Targeted and Efficient Model Stealing Defenses with Gradient Redirection. In *Proceedings of the International Conference on Machine Learning*, volume 162, 15241–15254.
- Orekondy, T.; Schiele, B.; and Fritz, M. 2019. Knockoff nets: Stealing functionality of black-box models. In *Proceedings of the IEEE/CVF conference on computer vision and pattern recognition*, 4954–4963.
- Orekondy, T.; Schiele, B.; and Fritz, M. 2020. Prediction Poisoning: Towards Defenses Against DNN Model Stealing Attacks. In *Proceedings of the International Conference on Learning Representations*.
- Papernot, N.; McDaniel, P.; Goodfellow, I.; Jha, S.; Celik, Z. B.; and Swami, A. 2017. Practical black-box attacks against machine learning. In *Proceedings of the 2017 ACM on Asia conference on computer and communications security*, 506–519.
- Redmon, J.; and Farhadi, A. 2018. Yolov3: An incremental improvement. *arXiv preprint arXiv:1804.02767*.
- Sanyal, S.; Addepalli, S.; and Babu, R. V. 2022. Towards data-free model stealing in a hard label setting. In *Proceedings of the IEEE/CVF Conference on Computer Vision and Pattern Recognition*, 15284–15293.
- Tramèr, F.; Zhang, F.; Juels, A.; Reiter, M. K.; and Ristenpart, T. 2016. Stealing Machine Learning Models via Prediction APIs. In *USENIX security symposium*, volume 16, 601–618.
- Truong, J.-B.; Maini, P.; Walls, R. J.; and Papernot, N. 2021. Data-free model extraction. In *Proceedings of the IEEE/CVF conference on computer vision and pattern recognition*, 4771–4780.
- Wang, Z.; Shen, L.; Liu, T.; Duan, T.; Zhu, Y.; Zhan, D.; Doermann, D. S.; and Gao, M. 2023. Defending against Data-Free Model Extraction by Distributionally Robust Defensive Training. In *Proceedings of the Annual Conference on Neural Information Processing Systems*.
- Yu, H.; Yang, K.; Zhang, T.; Tsai, Y.; Ho, T.; and Jin, Y. 2020. CloudLeak: Large-Scale Deep Learning Models Stealing Through Adversarial Examples. In *Annual Network and Distributed System Security Symposium*.
- Zhang, H.; Hua, G.; Wang, X.; Jiang, H.; and Yang, W. 2023a. APMSA: Adversarial Perturbation Against Model Stealing Attacks. *IEEE Trans. Inf. Forensics Secur.*, 18: 1473–1486.
- Zhang, H.; Hua, G.; Wang, X.; Jiang, H.; and Yang, W. 2023b. Categorical Inference Poisoning: Verifiable Defense Against Black-Box DNN Model Stealing Without Constraining Surrogate Data and Query Times. *IEEE Trans. Inf. Forensics Secur.*, 18: 1473–1486.

Implementation

Main steps. The reference distributions of all the classes are obtained once the target model is trained and remains unchanged afterwards. The detection module calculates the means and the covariance matrices with the updated window and then calculates the squared Fréchet distance. By comparing this distance to a properly chosen threshold, we can readily determine whether a query is malicious or not. Once a query is recognized as malicious.

Sliding window. For each account, we maintain a window of size N to store the encoder-extracted features of the latest queries. When an account a submits S images at a time for labeling, the encoded feature vectors of these images are pushed into its window to form an updated batch of features for calculating the feature statistics of each involved classes. Initially, the window is filled with N random samples from the target model’s training set to ensure that the target model preserves utility during the startup phase.

Detector threshold. Like other non-parametric detectors, we need to set an appropriate threshold τ to produce the final detection in the proposed defense module. To provide a feasible way to control the trade-off between utility and safety, we propose setting τ based on a specified tolerance level of performance degradation, which is measured by a dropping ratio γ in the testing accuracy of the D-ADD integrated target model. The testing accuracy increases gradually with the increase of τ , resulting in reduced impact of the defense module. When the threshold reaches a specific level, we obtain the maximum testing accuracy acc^* , which is the same as the original undefended model. We can then manage the service quality of the model after defense by specifying γ . As the preserved testing accuracy does not necessarily lead to the true utility, we may trade off less testing accuracy by setting τ to be slightly larger than the one that leads to the testing accuracy of $acc^* \times (1 - \gamma)$.

Experiments

Computing Infrastructure

All of the experiments are implemented by PyTorch 1.10 and conducted on a sever containing two NVIDIA GeForce RTX 4090 GPUs with 24GB RAM. The CUDA version is 11.2. The operation system of the server is Ubuntu 20.04 LTS.

Codes will be released once this paper is accepted.

Settings

Datasets. We trained five target models on MNIST, FashionMNIST, CIFAR-10 CIFAR-100, and Flower-17, and used another three datasets to simulate malicious or benign queries. Each involved datasets is summarized below.

- **MNIST.** This dataset consists of 70,000 grayscale images of handwritten digits (0-9), each of size 28x28 pixels. These images are split into two sets: 60,000 images for training and 10,000 images for testing. Each image corresponds to one of the ten digit classes.
- **FashionMNIST.** This dataset consists of 70,000 grayscale images of fashion-related items, designed as a more challenging alternative to the MNIST dataset. Each

image is 28x28 pixels in size and corresponds to one of 10 fashion classes. The dataset is split into a training set of 60,000 images and a test set of 10,000 images.

- **CIFAR-10 and CIFAR-100.** Both datasets (Krizhevsky and Hinton 2009) contains 60,000 32x32 color images that are split into two subsets with 50,000 for training and 10,000 for testing. CIFAR-10 consists of 10 classes of the same size, and CIFAR-100 is a more challenging variant of the CIFAR-10 that contains 100 equal-sized classes.
- **FLower-17.** This dataset contains 17 different species of flowers, with each class containing 80 images, resulting in a total of 1,360 images. The images vary in terms of size, orientation, lighting, and background.
- **Indoor-67.** This dataset contains 15,620 images belonging to 67 different indoor scene categories. Each category has at least 100 images collected from public sources such as Flickr and Google, with varying viewpoints, lighting conditions, and occlusions.
- **USPS.**
- **STL.**

Model architecture. Table A1 gives the model architecture used for each dataset. The same architecture is used for the clone model.

Malicious queries for KnockoffNets. For each target model, we follow (Kariyappa and Qureshi 2020) to use a different dataset (3rd column) as the surrogate data to simulate malicious queries in KnockoffNets attack.

architecture	training data	malicious queries (number)
Conv3	MNIST FashionMNIST	FashionMNIST (60,000) MNIST (60,000)
WRN-16-4	CIFAR-10 CIFAR-100	CIFAR-100 (50,000) CIFAR-10 (50,000)
ResNet-18	Flowers-17	Indoor-67 (15,620)

Table A1: Architectures of target models and surrogate set used as malicious queries

More results

Impact of window size on detection Fig. A3 plots the malicious scores of benign query batches (green dots) and malicious query batches (red dots) with various window sizes for MNIST and Flower-17. Results of other three datasets are presented in Fig. 3 of the main manuscript.

Limitation of PRADA. PRADA works effectively for adversarial attacks when the queries consist of natural seed images followed by perturbed visually similar ones. However, we found that it becomes ineffective when the queries combine natural surrogate images with in-distribution samples.

We plotted the detection results of PRADA in Fig. A1 when a malicious account attempted to steal MNIST and CIFAR-10 classification models using FashionMNIST and

CIFAR-100 samples as surrogate queries, respectively. This figure shows that it is difficult to distinguish malicious queries from benign ones. Although the Shapiro-Wilk scores of malicious histograms are smaller than the benign ones, the gap is subtle. We get similar results in in Fig.A2 when histograms are calculated with queries containing both surrogate and in-distribution samples, showing that PRADA is insensitive to the distribution difference of natural image queries even when the mixing ratio is as large as 30%.

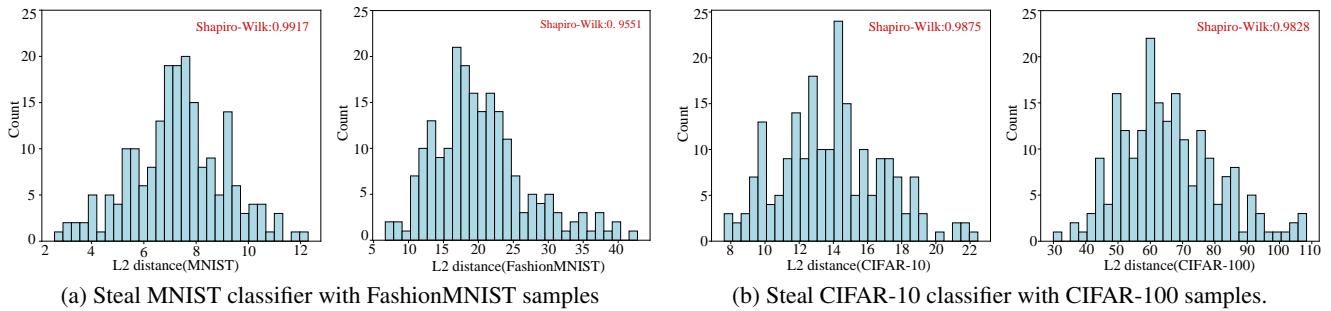


Figure A1: Comparison of the normality of distribution of distances produced with PRADA between **benign** queries (on the **left**) and **malicious** queries (on the **right**). The KnockoffNets stealing attack is simulated by using FashionMNIST and CIFAR-100 to query the classification model trained on MNIST and CIFAR-10, respectively. The Shapiro-Wilk score ranged in $[0, 1]$ measures the fitness of a set of values to a normal distribution.

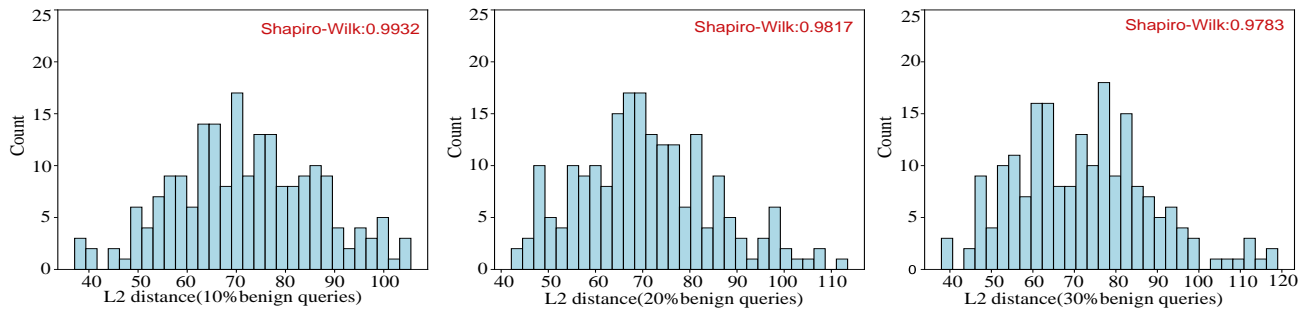


Figure A2: Histograms produced by PRADA with mixed surrogate/OOD (CIFAR-100) and in-distribution (CIFAR-10) images. The in-distribution percentage is 10%, 20% and 30%, respectively.

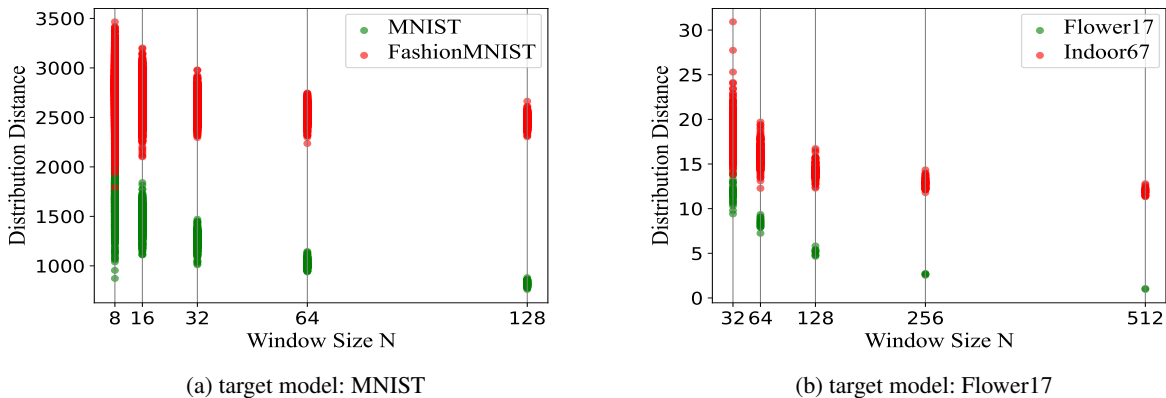


Figure A3: Impact of sliding window size N on distribution of Malicious Score (MS)s. Each red dot is calculated with a window of N randomly selected surrogate samples as malicious queries, and each green dot is calculated with N randomly selected testing images as benign queries.